

STUDY OF DRUG FORCE AND THE FLOW FIELD ON ROAD VEHICLES

Khalid M. Sawoud

Assistant lecturer, Automotive Engineering Department /Technical Collage-Baghdad

E-mail: khalidreem90@yahoo.com

(Received: 1/12/2013; Accepted:2 /2/2014)

ABSTRACT: - Improving road vehicles performance needs to deep understanding the science of aerodynamics, in order to control flow field by means of active and passive control techniques. The airflow behavior when passes over the road vehicles surfaces will be changes in patterns and resulting in different pressure regions. This pressure region causes drag force and thereby increases in fuel consumption of the road vehicles.

This paper include experimental study to investigate the effect of road vehicles for three most common rear end configurations design such as (square, notch and fastback) on drag force, drag coefficient and pressure distribution. The experiments were carried out an open, low speed, and three dimensional wind-tunnel, on geometrical similarity to the prototype (Audi 80 1987) in scale down (1:18) wooden models for four different velocities (11.31, 13.86, 17.89 and 22.98) m/sec.

The results obtained from the wind-tunnel investigations showed that the drag force increases with the increasing of free-stream velocities. The minimum drag coefficient can be achieved with fastback configuration, comparing with the other tested models and result in approximately 16% and 48% lower than that for notch and square back configurations, respectively. These results are demonstrated by the pressure distribution curves which provide a deep understanding of the flow behavior above the tested models.

Keywords: Wind-tunnel, Drag force, Aerodynamics, Road vehicles.

NOMENCLATURE

Symbols	Description	Units
D	Drag force	N
C_d	Drag coefficient	-
C_p	Pressure coefficient	-
Re	Reynolds number	-
V_∞	Free stream velocity	m/s

STUDY OF DRUG FORCE AND THE FLOW FIELD ON A ROAD VEHICLES

A	Projected model cross section area	m ²
W	Counterbalance weight	Kg
d ₁	Drag force arm	m
d ₂	Weight arm	m
ρ	Free stream fluid density (For air and water at STP 1.225 and 1000, respectively).	kg/m ³
μ	Dynamic viscosity (For air at STP 1.78×10 ⁻⁵).	N.s/m ²
h _{T∞} - h _{S∞}	Pitot-static tube reading	cm.H ₂ O
P _{SL}	Local static pressure	cm.H ₂ O
P _{S∞}	Free stream static pressure	cm.H ₂ O

SUBSCRIPTS

S _L	Local static pressure on the model surface (taps reading)
S _∞	Free-stream static pressure
T _∞	Total Free-stream pressure

1. INTRODUCTION

The studies of external flows around the bodies have a great importance in many engineering applications. Safe design, handling and performance of airplanes, ships, missiles, compressors, turbines, trains, and automobile bodies can benefit from a general understanding of these flows, different forces and moments associated with this flow around bodies.

In automobiles aerodynamics and specially the subject of drag reduction have more important in recent years due to the rapidly increasing in fuel prices and exhausting resources. In road vehicles as an aerodynamically well designed can spends the least power in overcoming the drag exerted by air and hence exhibits higher performance-cruises faster and longer, that too on less fuel ⁽¹⁾. For better fuel economy, greater vehicle performance and improvement the road holding and stability in move, has prompt the aerodynamicist to exert a lot of researches on the flow field and drag reduction for different body shapes and speeds.

When the road vehicle is moving at an undistributed velocity in a fluid stream, a force is exerted on the road vehicle which may be inclined to the flow direction. This force is called aerodynamic force and represents the sum vector of two forces, first, tangential force (shear-stress force) result due to effect viscosity and velocity gradient at surface boundary-layers, secondly, normal force result due to difference in pressure distribution around the road vehicle surfaces. Component of this force parallel and opposite to the direction of flow past the road vehicle body is known as aerodynamic drag (resistance force) ⁽²⁾.

Aerodynamic drag force is the force acting on the vehicle body resisting its forward motion, and split into two main types, skin friction drag (induced drag) which is related to the project area and form drag (pressure drag). The pressure drag force is an important force to

be considered while designing the external body of the vehicles, since it covers about 65% of the total force acting on the complete body⁽³⁾.

The major factors which affect the flow field around the vehicle are the formation of boundary layers, separation of flow field; friction drag and lastly the pressure drag ⁽⁴⁾. Separation and reattachment are the particular interest when study the external flow. Separation occurs when the mean stream separates from the surface of the body, and causes large drag. Separation may result from a stream wise pressure increases or effect of the rear end of the road vehicles curvature.

One of the main causes of the base drag force in road vehicles is the separation of flow near the vehicle rear end and formation wake zone at downstream. To delay flow separation and consequently minimize the wake zone, boat- tailing and tapering the rear end configuration can result in a considerable drag reduction.

Numerous investigations have been reported on base drag reduction of automobiles over few decades. Dheeraj S., Akshoy R., Ravi R. and Anuj J. ⁽⁵⁾, studied the effect of spoiler combination with the vortex generators on the (SEDAN) drag and found that a best combination with flow angle=0 deg. And with rear spoiler at angle=45deg. resulting in drag coefficient reduction with impressive 68%. Ahmed S. R. ⁽⁶⁾, investigated the effect of the slat angle of upper rear surface of vehicle on (Hucho, 1975; Morel1978; Ahmed 1984), they found that the net drag reaches a minimum value at ($\alpha=15\text{deg.}$), where the slant angle is that measured from the horizontal. M. Hassan Ali, Mohammad Mashed, Abdullah Al Bari and Muhammad ⁽⁷⁾, studied the effect of install (VGs) immediately upstream of the flow separation point in order to control separation of air flow above the sedan's rear end and resulting in a considerable drag reduction.

The lift force (L), which represents the aerodynamic force component that acts in normal direction to the airflow. These force produced due to the pressure distribution on the lower and upper surfaces of the road vehicles. Since the present study was limited to observations and change in static pressure along the upper surface centre line of the road vehicle and because of the limitations of single-component balance device that built under the wind tunnel test section and used to measure force on single axis in the direction parallel to the length of the model only which led to the inability to calculate the lift forces.

In present study, we have explored the effect of rear end configuration on the drag force and the flow field of the automobiles, since rear end shape has a major effect on the total drag and can also is responsible up to 35% of vehicles drag, which is more than the influence of front body. It is very important to find a proper shape of rear body surface which brings the divided stream line smoothly together, as shown in figure (1) ⁽³⁾. The carried investigation to show which shape are aerodynamically best at reducing the drag force.

2. EXPERIMENTAL SET-UP

In this paper, the experimental tests were carried out in an open circuit, low speed, and three-dimensional suction type wind-tunnel. The transparent test section made out of glass with dimensions (40×35×35) cm, as shown in figure (2), the air through which has drawn by 12-blades fan which are rotated by 8hp variable speed electric motor, and the free stream velocity was measured by Pitot - static tube placed at the entrance of the test section. The tested velocities were varied 11.31, 13.86, 17.89 and 22.98m/sec, given a corresponding Reynolds number ranging between $(0.68 - 1.27) \times 10^5$ (based on the model length).

The experiment were carried out using three popular shapes on a geometrically similar and in scale down (1:18) wooden models, as shown in figure (3). They are different from the prototype (Audi 80 1987) only in size. To achieve the dynamics similarity, it is required to build a full scale. The model dimensions turned out to be very large compared with the dimensions of the test-section. In order to avoid the blockage effect, so the scale has been chosen carefully based on the test-section size of tunnel was made keeping in view the percentage blockage is less than 7.5% ⁽⁸⁾. A cross-section area of 80cm² was maintained for all tested models. In present work, the free stream velocity, drag force and pressure variations are measured as follows:

- 2-1. The free stream velocity (V_{∞}) was measured by inserted a Pitot-static tube from the wind tunnel roof into the inside and at the test-section center line, as shown in figure (4).
- 2-2. Drag force of the experimental model was measured indirectly by using a single component balance device, as shown in figure (4). For mounting the experimental model on the balance, a vertical aerodynamic strut was fabricated especially for this purpose with length (460×5×1) cm. The drag force generated on the tested model is balanced by weights placed on. This device has many advantage such as kept outside the test-section, hence, don't disturb the flow. Installation details of the single component device with the model are shown schematically in figure (5).
- 2-3. To measure the local static pressure variation on the model upper surface, there are 10 pressure taps 0.9mm diameters, each one inserted in a small 10 holes 1mm diameter were drilled on the axis-symmetric line with interval ($\theta=20^\circ$). The pressure tap locations at which pressure were measured are indicated in figure (6). The present investigation was done with an objective with the following experimental procedure:

The free stream velocity calculations are done by using the equation (1) ^(9, 10):

$$V_{\infty} = \sqrt{\frac{2[\rho_{\text{water}} \times g \times (h_{T\infty} - h_{S\infty})]}{\rho_{\text{air}}}} \quad \text{----- (1)}$$

And the corresponding Reynolds number is calculated using equation (2)^(9, 10):

$$R_e = \frac{\rho V d}{\mu} \quad \text{----- (2)}$$

The drag force and local static pressure measurements are taken as follows:

- a) The first model (square back) configuration was mounted in the wind tunnel test-section on aerodynamic strut and then to single component balance device which placed under the wind tunnel test section. It was not in any way touch the test-section walls, otherwise, the wind tunnel vibrations will be transmitted to the balance device and causing undesirable reading.
- b) The Pitot - static tube and pressure taps connection to the multi-tube manometer was checked.
- c) The wind tunnel will be operated and the speed adjusted to the first speed 11.31m/s and for five minutes allowed to get steady and uniform flow.
- d) The model will be moved down due to effect of drag force. In order to counterbalance these force adding the dead weight to the balance device until the model came back to the level position and then recorded the amount of weight which counterbalance the drag force. By taking the moment about the pivot point (B), we get the drag force (D):

$$D \times d_1 = W \times d_2 \quad \text{----- (3)}$$

Drag force (D) values for notchback, fastback and square back at the tested velocities are calculated by equation (3) and are given in Table (1).

The drag coefficient (C_d) is calculated by using equation (4)^(9, 10) below:

$$C_d = \frac{F_D}{\frac{1}{2} \rho V_{\infty}^2 A} \quad \text{----- (4)}$$

The drag coefficient (C_d) values for notchback, fastback and square back at the tested Reynolds number are calculated by equation (4) and listed in Table (2).

- e) The local static pressure from multi-manometers was observed and recorded in (cm-H₂O).

The pressure coefficient (C_p) is calculated by using equation (5)^(9, 10) below:

$$C_p = \frac{P_{st} - P_{s\infty}}{\frac{1}{2} \rho V_{\infty}^2} \quad \text{----- (5)}$$

- f) The wind tunnel speed will be increased to 13.86m/s and repeated the steps (c, d and e) and recording the above readings for the second speed. Repeat the same steps for the third and fourth speeds 17.89 and 23.98m/s, respectively.
- g) Similar measurements were done for the notch and fast back configurations, by repeating the steps (a, b, c, d, e, and f).

3. DATA REDUCTION

- i. Pitot - static tube- By applied the Bernoulli's equation locally to convert the dynamic pressure to local stream wise velocity component, equation (2).
- ii. Drag force-convert the dead weight counterbalance to the drag force by taking the momentum about the pivot point, and then to the drag coefficient, equation (4).
- iii. Surface Pressure Distribution-Convert the measured static pressure differences (in cm.H₂O) and free stream dynamic pressure to local pressure coefficient (C_p), equation (5).

4. RESULTS AND DISCUSSION

4-1. Pressure coefficient

The figures (7, 8, and 9) show the trend of pressure distribution by means of dimensionless pressure coefficient (C_p) along the centerline and mid plane of the upper surface of the scaled models (square, notch, and fast back) configurations, respectively. The results show that the distributions of C_p are practically similar for all the tested model configurations, and at the tested velocities. From the figures it is observed that the pressure at the front (tap No.1) is represent the stagnation point which gives a positive pressure region ($C_p = 1.0$), and then the air stream flow accelerated from the bonnet leading edge to its rear half which gives negative pressure coefficient, and the flow become slower from the bonnet rear half to the mid-front windscreen region, which are gives positive pressure coefficient. While the airstream speed is at highest values over the rear end of the front windscreen and roof (taps No.4 and 5) which gives a large suction pressure and reached the peak values ($C_p = -1.5$ to -1.7) at the reattachment region of the boundary layers.

Comparison between the pressure coefficient for the three models square, notch and fast back configurations at three different speeds ,indicates that the flow stream separation at the model upper surface and especially at the rear end (indicated by taps No.9 and 10).

For the square back configuration, when the rear end surface having a sharp inclination, the boundary layers and its interaction with the local pressure gradient plays a significant affecting in the flow over the rear end and causes the flow to separate at the top of rear end resulting in a low negative pressure (negative pressure coefficient) and causes a large wake zones behind it. It's evident that from figure (7) the whole base area is subjected to negative pressure.

For notch back model, with a stepped rear end body. The separates airstream over the rear roof edge and due to downwash causes it to reattach itself to the body downward near to the edge of boot, the pressure coefficient rises over the base, and resulting in wake zone in smallest size compared with that in square back configuration, as shown in figure(8).

The optimum shape among the tested models is the fast back, where the pressure gradient changes from being negative to positive pressure (increasing pressure), indicating that the boundary layers separation occurs further downstream on the rear end than that for the square and notch back configurations. This resulting in smallest size of the wake zone and consequently in low drag force, as shown if figure (9).

4-2. Drag force

Figure (10) shows that the variation of drag force (F_D) with the free-stream velocity for the three different models (square, notch, and fastback) configurations, the behavior of curves are identical to that in theoretical, it is increases as the free-stream velocity increased, and this can be attributed to the boundary layer thickness adds to the effective thickness of the tested model which leads to increase the pressure drag. It is interesting to observe that the drag force for fast back configuration at tested velocity 11.39 m/sec is lower than that for square and notch back in 86 percent and 24 percent, respectively. These percentages decreased with increasing the velocity and become 18 percent and 9% percent at free stream velocity 23.98m/sec. This can be attributed to the fact that the fastback is more streamline in the profile in the rear portion so the separating streamlines occurs at the lowest point of the rear end and the wake is correspondingly smaller resulting in low drag force.

4-3. Drag coefficient

Figure (11) shows the variation of drag coefficient C_D with the free-stream velocity for different three model configurations. It is very clear that the value of C_D for the square back is greater than that for notch back and fast back configurations, and this value of drag coefficient decreases as the free-stream velocity increases. This can be attributed to the boundary layer separation. Since also it is a noticeably that the square back has mean drag coefficient (0.71) greater than the notch back (0.51) and fast back (0.45) at the same free stream velocity ($V_\infty=22.98\text{m/s}$).

Figure (12) shows the variation of drag coefficient C_D with the Reynolds numbers for each configuration. It is clearly evident from the figure that the drag coefficient is inversely proportional to Reynolds number which is decreased with increased in Reynolds number. According to the present results, the maximum drag coefficient 0.9 and 0.56 occurs at

$Re=0.62 \times 10^5$ for square back and notchback, respectively, whereas, for fastback is 0.48. These values are reduced as the Reynolds number increased ($Re = 0.72 \times 10^5$, 0.98×10^5 and 1.27×10^5), as shown in figure (12) and this refer to flow pattern where separated boundary layers take place further downward along the rear end surface than before.

5. CONCLUSION

From the data and analysis of results undertaken in this study considering the effects of the rear end configuration on the flow field and drag force for road vehicles, it is possible to conclude the following:

- 1- The fastback configuration has a mean drag force less than that for square back and notchback configuration in 16% and 48%, respectively. This due to the difference in shape especially in the rear back. In fastback the rear portion profile is most aerodynamically shape.
- 2- The results obtained were very confirmed with the theoretical understanding of variation of drag force, drag coefficient with the air velocity and Reynolds number.

REFERENCES:

- 1) M. Desai, S. A. Chaniwala, H. J. Nagarsheth, (2008), "Experimental and Computational Aerodynamic Investigations of a car", WSEAS Transaction on Fluid Mechanic, Issue 4, Volume3.
- 2) P. N. Krishnani (2009), "CFD studies of Drag Reduction of a Generic Sport Utility Vehicle", M.Sc. Thesis in Mechanical engineering, California State University, Sacramento,
- 3) H. Heinz, (1989), "Vehicle Body Aerodynamic", Second Edition, A. Edward, pp584-634.
- 4) M. Desai, S. A. Chaniwala, H. J. Nagarsheth (2008), "Computational Validation of Experimental Aerodynamics predictions of a Car", 6th International conference on Fluid Mechanics and Aerodynamics. Rhodes, Greece.
- 5) S. Dheeraj, R. Akshoy, R. Ravi and J. Anny, (2010), "Aerodynamic Effect of Rear Spoiler and Vortex Generators on Passenger Car", International Conference on Theoretical, Applied, Computational and Experimental Mechanics, IIT Kharagpur, India.
- 6) S. R. Ahmed, (1984), "Influence of Base Slant on the Wake Structure and Drag of Road Vehicles", Trans. ASME, J. Fluid Engineering, 105:429-34.
- 7) M. Hassan Ali, Mohammad Mashud, Abdullah Al Bari and Muhammad" Aerodynamic Drag Reduction of a car by Vortex Generation", Int. Journal of Mechanical Engineering, Volume 2, Issue 1, ISSN: 2277-7059.

- 8) Cengel, M. John and Yunas A. Cimbala, (2006), "Fluid Mechanics Fundamental and Applications", McGraw Hill, New York.
- 9) J. Anderson, (2005), "Fundamentals of Aerodynamics", Third Edition, McGraw-Hill.
- 10) S. F. Horner, (1965), "Fluid Dynamic Drag". Midland Park, NJ.
- 11) T. Tsutsui, and T. Igarashi, (2002), "Drag Reduction of a circular cylinder in an air-stream". Journal of Wind Engineering International Aerodynamics, 527-541.
- 12) W. H. Hucho, (1998), "Aerodynamic of Road Vehicles", 4th Edition, Society of Automotive Engineers (SAE), Warren dale, USA.
- 13) A. Wittor and S. Moller, (2002), "Characteristic of the low speed wind tunnel of the UNNE", Journal of Wind Engineering and Industrial Aerodynamics, pp 307-320.
- 14) G. Buresti, (2000), "Bluff-body Aerodynamics". Lecture Notes, Department of Aerospace Engineering University of Pisa, Italy.
- 15) W. Stapleford, (1981), "Aerodynamic Improvements to the Body and Cooling System of a Typical Small Saloon Car", Journal of wind Engineering & Industrial Aerodynamics, Vol.9, pp 63-75.
- 16) K. M. Sowoud and E. Radhakrishnan, (1991), "Passive device for base drag reduction", proceeding of the 18th National conference on Fluid Mechanics and Fluid Power, Indore, India. pp (G25-34).

Table (1): Drag Force for Tested Models.

Trial No.	Velocity(m/s)	Drag Force(N)		
		Notchback	Fastback	Square back
1	11.31	0.36	0.29	0.54
2	13.86	0.50	0.44	0.68
3	17.86	0.83	0.72	0.98
4	22.98	1.20	1.10	1.30

Table (2): Drag Coefficient for Tested Models.

Trial No.	Reynolds Number (Re)	Drag Coefficient(C _D)		
		Notchback	Fastback	Square back
1	0.62E+5	0.56	0.48	0.90
2	0.76 E+5	0.52	0.47	0.72
3	0.98 E+5	0.51	0.46	0.62
4	1.27 E+5	0.46	0.43	0.50

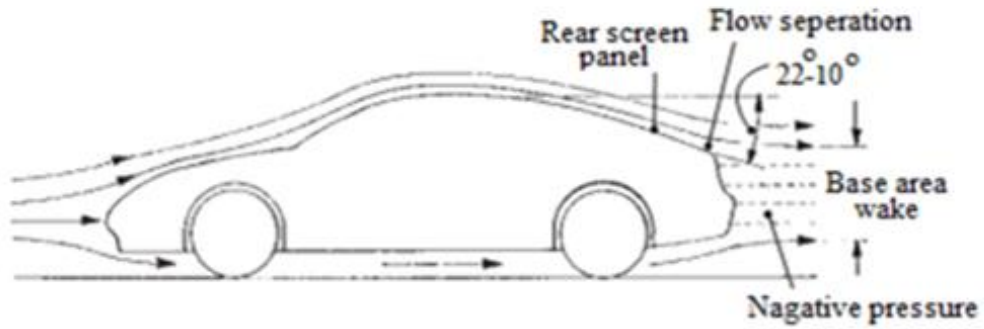


Fig.(1): Design of Road Vehicles Rear End Configuration (3).

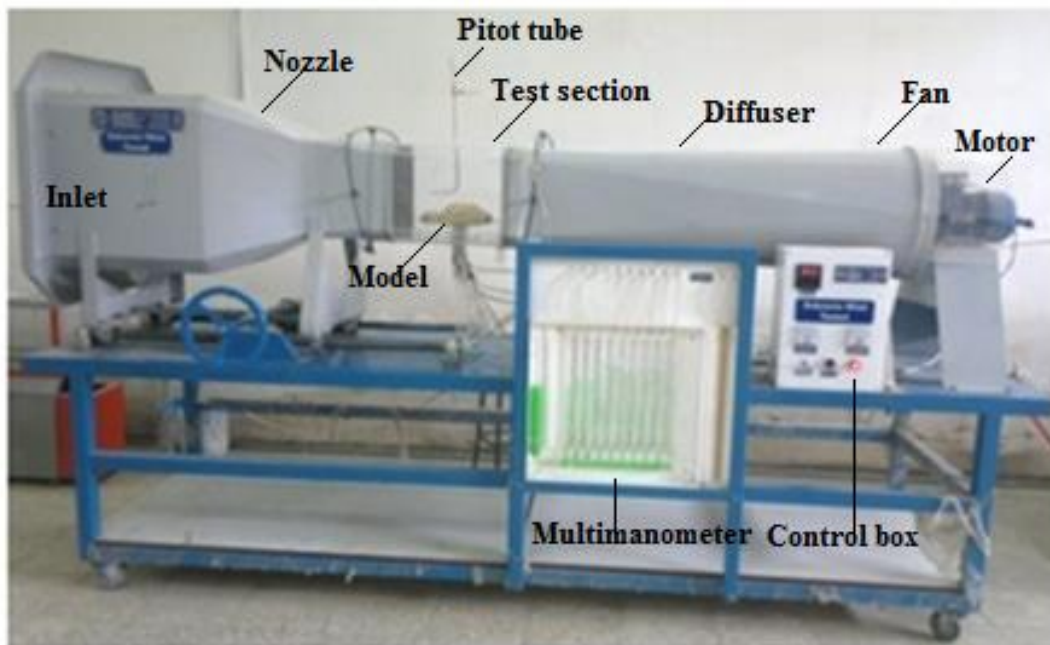


Fig.(2): Experimental Set-up.

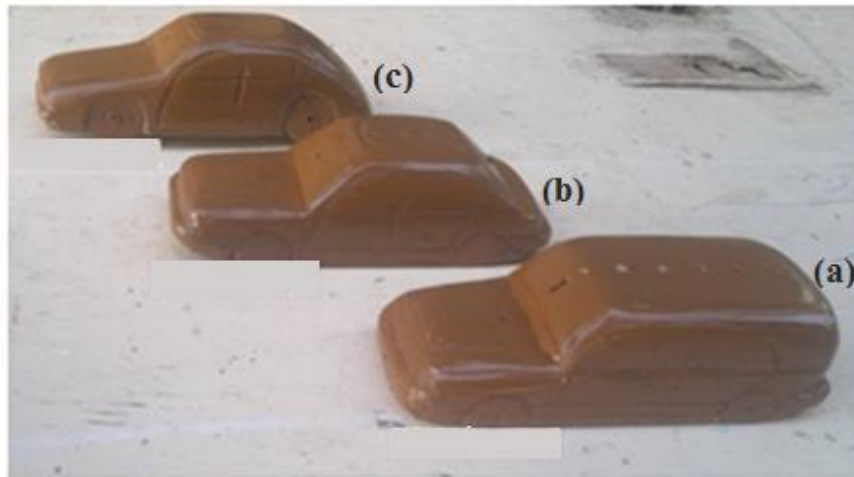


Fig.(3): Experimental Models (a)Squareback, (b)Notchback and (c) Fastback.

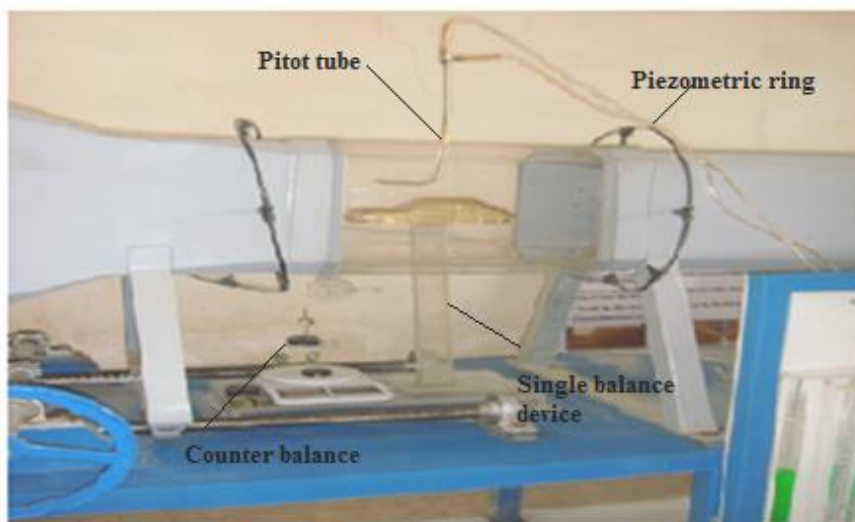


Fig.(4): Wind-tunnel Test Section with Single Component Balance for Drag Force Measurements.

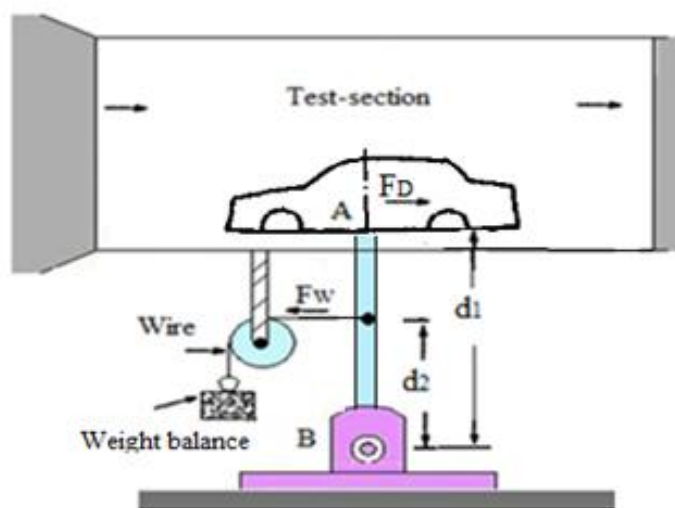


Fig.(5): Installation Details of the Single Component Balance Device.

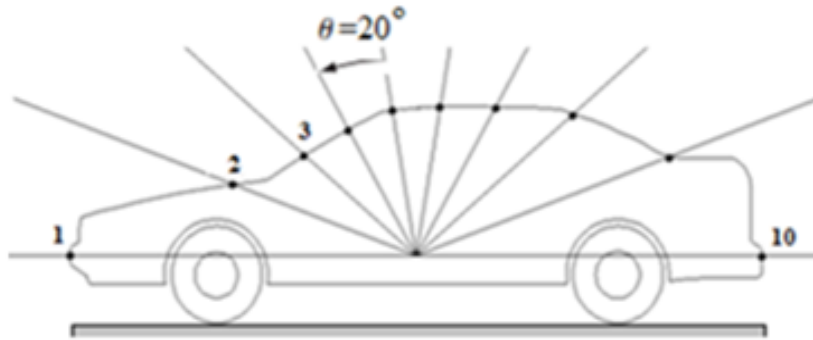


Fig.(6): Tested Model with Pressure Tapping.

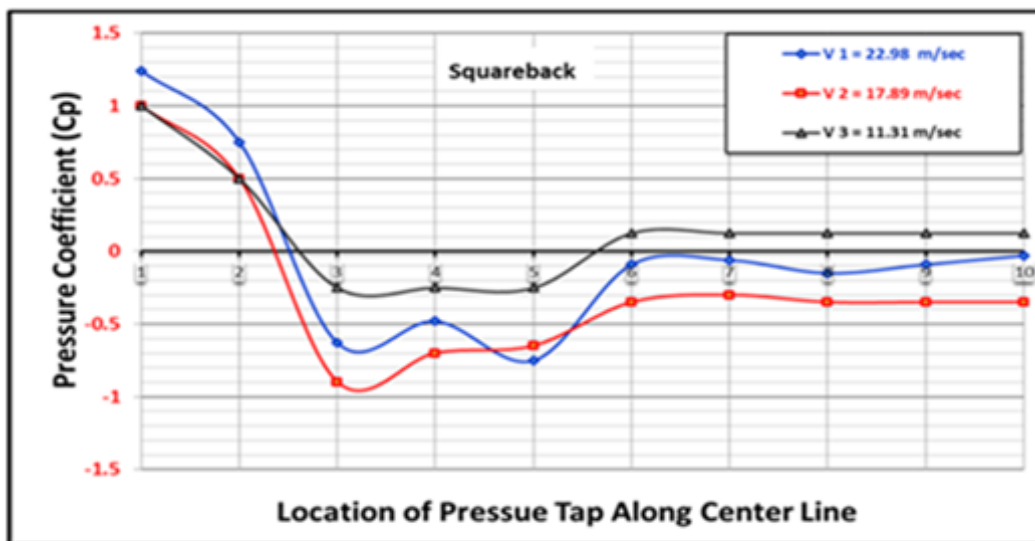


Fig.(7): Variation of Pressure Coefficient (Cp) along the Center Line of Squareback Configuration and for Different Three Velocities.

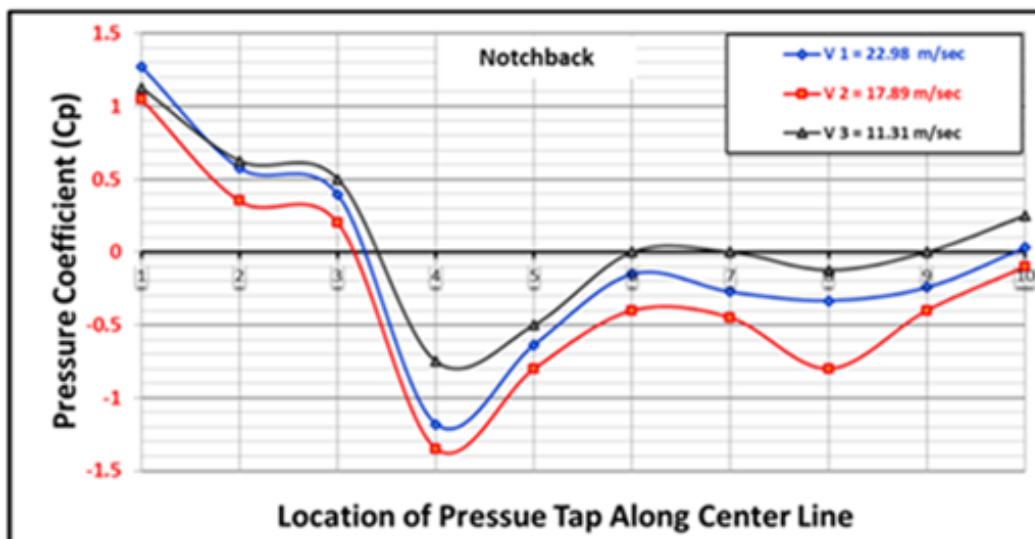


Fig.(8): Variation of Pressure Coefficient (Cp) along the Center Line of Notchback Configuration and for Different Three Velocities.

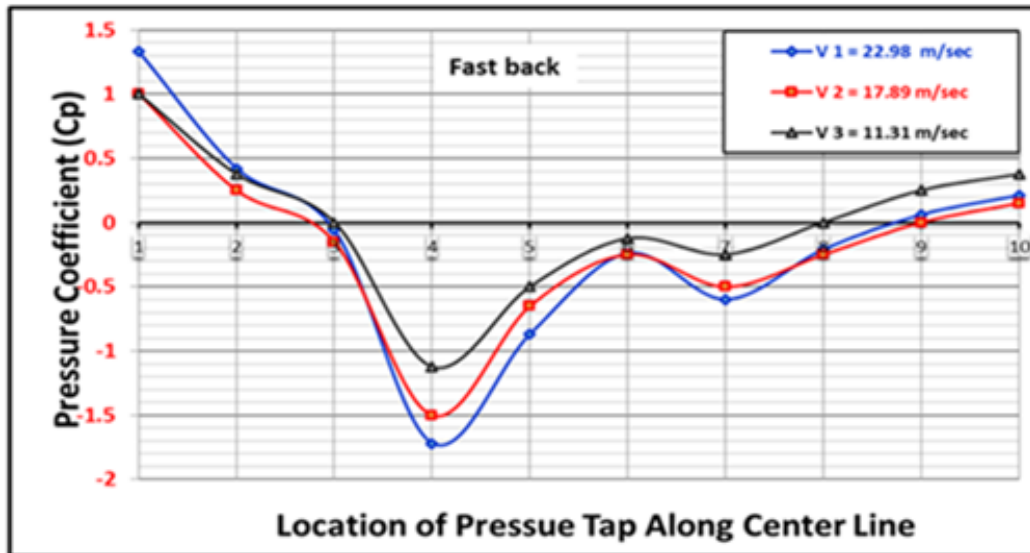


Fig.(9): Variation of Pressure Coefficient (Cp) along the Center Line of Fastback Configuration and for Three Velocities.

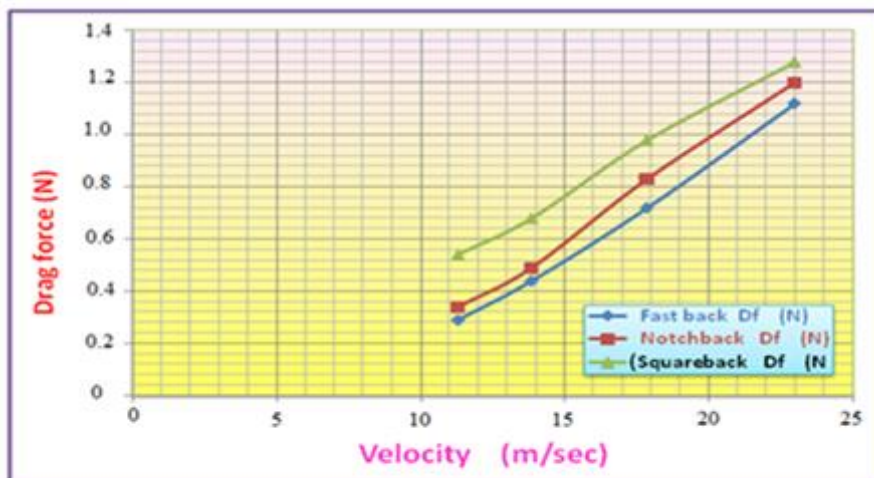


Fig.(10): Drag Force Variation with Velocity for the Three Configurations.

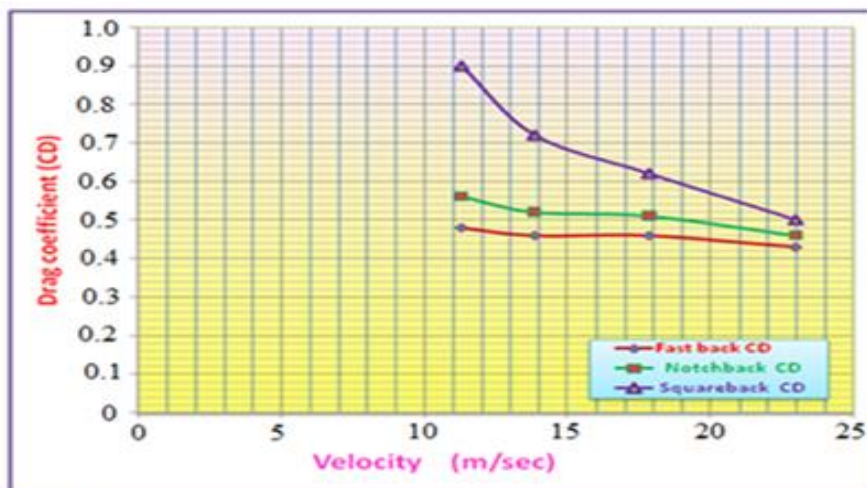


Fig.(11): Drag Coefficient (CD) Variation with the Free stream Velocity for the Different configurations.

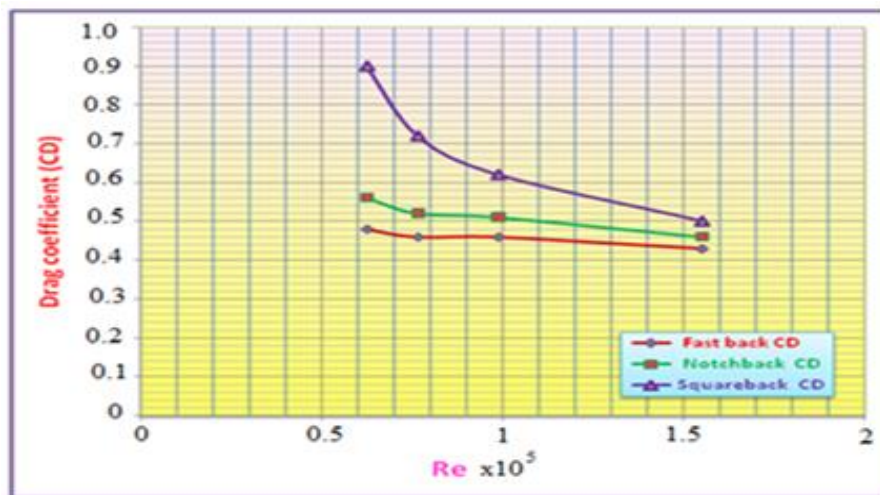


Fig.(12): Drag Coefficient (CD) Variation with Reynolds Number for the Different Three Configurations.

دراسة قوى الكبح ومجال الجريان على مركبات الطريق

خالد مصلح سعود

مدرس مساعد / الكلية التقنية الهندسية-بغداد

الخلاصة:

ان تحسين أداء مركبات الطريق يحتاج الى فهم عميق لعلم الايروداينمك، لغرض السيطرة على حقل جريان المائع وذلك من خلال استخدام تقنيات خاملة أو فعالة. أن نمط جريان الهواء عند مروره فوق سطح مركبات الطريق سوف يتغير وينتج عن ذلك مناطق ضغط مختلفة الشدة. وأن هذه المناطق سينتج عنها قوى كبح وبالتالي سوف تزيد من أستهلاك الوقود لمركبات الطريق.

ان هذا البحث يتناول اجراء فحوصات تجريبية لتأثير شكل النهاية الخلفية ولاكثر ثلاثة أنماط شيوعا في تصميم زاوية منحدر النهاية الخلفية (النموذج الاول الذي تكون له زاوية منحدر للنهاية الخلفية تتراوح بين 90- 50 درجة، النموذج الثاني ذات النهاية المتدرجة واما النموذج الثالث الذي تكون له زاوية منحدر للنهاية الخلفية أقل من أو تساوي 25 درجة) لمركبات الطريق على قوى ومعامل الكبح وكذلك على توزيع الضغط الأستاتيكي. أن الفحوصات التجريبية قد نفذت باستخدام نفق هوائي، ذات مدى سرعة واطئة، دون الصوتية، ومن النوع المفتوح على النماذج المختبرية والمشابهة هندسيا للنموذج الأصلي (سيارة أودي-80-موديل 1987) وبنسبة تخفيض (1:18) والمصنعة من الخشب ولسرعة مختلفة (11.31, 13.86, 17.86 و 22.98) متر لكل ثانية.

أظهرت النتائج والبيانات التي تم الحصول عليها من اختبارات النفق الهوائي أن قوى الكبح تزداد مع أزيد سرعة جريان الهواء. ان أقل معامل كبح تم الحصول عليه للطراز الثالث (Fastback), وبمقارنته مع النماذج الاخرى أظهرت النتائج بأن له معدل معامل قوى كبح أقل بحدود 16% و 48% من قوى الكبح للطراز الاول (Notchback) والثاني (Square-back)، على التوالي. أن منحنيات توزيع الضغط التي تم الحصول عليها تبرهن صحة النتائج وتساعدنا على فهم سلوك جريان الهواء حول النماذج التي تم فحصها.

الكلمات المفتاحية: قوى الكبح، مركبات الطريق.